Real Time Indicators of Material Refinement in an Attritor Mill

Priya R. Santhanam and Edward L. Dreizin
Otto H. York Dept. of Chemical, Biological, and Pharmaceutical Engineering, New Jersey Institute of Technology, Newark, NJ 07102

DOI 10.1002/aic.13897
Published online August 20, 2012 in Wiley Online Library (wileyonlinelibrary.com).

Power, torque, and rotation speed of the impeller of an attritor mill were measured during preparation of metal matrix composite powders. Compositions of Al·MgO and Al·B_4C were selected to include ductile (Al) and brittle components. Brittle components, MgO, and B_4C, were respectively softer and harder than the milling media (hardened steel). Yield strength of pressed powder compacts and x-ray diffraction peak width were treated as indicators of the achieved structural refinement. Both peak width and yield strength increased for both materials at longer milling times. Torque and power increased for Al·MgO but decreased for Al·B_4C at longer milling times. The results were interpreted considering differences in hardness of MgO and B_4C. Amplitudes of rapid oscillations of the milling process parameters were also monitored and were observed to correlate with the material refinement. Utility of real-time milling progress indicators for different types of materials is demonstrated. © 2012 American Institute of Chemical Engineers *AIChE J,* 59: 1088–1095, 2013
Keywords: mechanical milling, mechanical alloying, milling progress, metal matrix composites

Introduction

Mechanical milling is widely used for the preparation of various advanced materials.[1] Material is refined and modified as a result of multiple interactions with milling balls occurring at different impact energies and configurations. Most commonly, the milling progress is assessed by recovery of partially milled samples at regular time intervals. Such samples are evaluated based on their particle sizes, shapes, crystal structures, or mechanical properties to establish the time necessary to prepare the required material.[2–4] This approach is labor-intensive, and more streamlined methods capable of quantifying the milling progress are desired.

In the past, several research groups have realized the difficulty in tedious evaluations of partially milled samples and identified alternative ways of assessing the milling progress. Some of the parameters proposed to track the milling progress include power consumption and torque from the motor attached to the mill,[5–8] temperature inside the milling vial,[6,9,10] vial vibration frequency and amplitude, and frequency of ball impacts.[11] In addition, visualization of the ball motion and analysis of the recorded high-speed videos was discussed.[12]

One of the early attempts to use real-time diagnostics was by Goodson et al.,[5] who used Charles equation correlating the specific energy input to the mill E [kW·h/kg], and median particle size d_p [μm], as $E=Ad_p^{\alpha}$, where A and α are parametric constants. The experiments were carried out using a laboratory attritor with a mixture of tungsten carbide and cobalt powders. The specific energy input, E, was obtained from the power draw for the mill. After milling, the powder samples were pressed and vacuum sintered. The density, coercivity, Rockwell hardness, and specific magnetic saturation of milled and sintered cylinders were measured as functions of milling time. Charles equation was shown to describe the experimental results. However, it reduced the effect of milling conditions to one fixed parameter, energy input to the mill, which may not hold true for a broader range of milling conditions. The value of E can change when the properties of the milled material evolve, although preset milling parameters remain fixed. Further, parameters A and α certainly are material-specific and, for some materials, they may not remain constants while properties of the materials being milled change as a function of the milling time.

Kimura and Takada[6] set up a data acquisition system on a custom rotating arm ball mill (similar in operation to the attritor mill used in this work). Apart from the torque on the rotating arm, the temperature inside the vial was also monitored as a function of milling time. The aim was to track a solid state amorphization transformation in Co-Zn alloys. The measured torque was established to be sensitive to changes in powder structure, whereas the attrition temperature was proposed to be a direct indicator of the kinetics of solid state amorphizing transformations. Thus, utility of tracking torque and temperature as real-time indicators of milling progress was shown. Extension of these results to other materials systems and correlations between the changes in torque and temperature on one hand, and properties of the milled material systems, on the other hand, became of substantial interest.

Temperature measurement was also considered as a reaction progress monitor in some of the earlier projects from the present research group.[9,10] The systems under consideration included mechanically alloyed Al-Mg powders as well as materials capable of highly exothermic reactions. Both

Correspondence concerning this article should be addressed to E. L. Dreizin at dreizin@njit.edu.

shaker and planetary mills were instrumented to read out the vial temperature. For the mechanically alloyed powders, the temperature measurement was useful in establishing different stages of the milling process, for example, formation of flake-like particles, breaking down the flakes, and formation of composite and then alloyed powders.[13] For the exothermically reacting materials, as is common in reactive milling,[14] the temperature jump in the milling vial may show directly and very clearly when the reaction has occurred.

Mulas et al.[11] employed a piezoelectric transducer and magnetic position sensor to measure impact frequency, impact time and vial velocity in a single-ball vibro-mill and a shaker mill. The primary objective was to establish the right amount of energy and thereby, milling parameters necessary to initiate a self-propagating reaction in the materials system of interest.

Iossanna and Magini[7,8] reported electrical and mechanical power consumption measurements on a planetary mill in their two successive articles. Their work stemmed from the interest in comparing the theoretical energy consumption in a ball milling process predicted by on mechanistic collision models to that obtained from experimental power consumption measurement. The authors established a satisfactory correlation between the two for a planetary ball mill and suggested that the same concept could be extended to other devices.

In summary, the utility of the real-time measurements of the consumed power, vial temperature, and some of the other characteristics of the milling process has been well established. Most successful real time measurements indicated qualitative changes in the material properties, such as formation or destruction of flakes and occurrence of exothermic, self-sustaining chemical reactions. However, detection of more subtle changes in the materials properties, for example, evolution of the particle sizes, development of the alloyed phases, altering mechanical strength and hardness, has proven to be more challenging. All related measurements were performed for individual materials systems and customized milling configurations. Thus, it remains unclear whether such trends, identified rather narrowly for specific materials systems and milling devices, are capable of predicting milling progress for different materials or different milling configuration.

It is interesting that many related efforts involved shaker and planetary mills, devices that are very common in laboratory experiments, but not readily scalable for commercial manufacturing. Conversely, the data on correlations between real-time power consumption and torque and material refinement in the attritor mills are very difficult to find, whereas attritors are most likely to be used in larger scale production of new materials. This lack of data for attritor mills is especially surprising considering that some of the popular commercial attritor mill models, for example, by Union Process, are routinely equipped with sensors and a data acquisition board, enabling users to read and record power, rotation rate, and torque readily.

This project is aimed to establish an experimental foundation for assessing milling progress while preparing materials in an attritor mill utilizing noninvasive, real time process indicators. A systematic approach is proposed, relying on simultaneous measurements of the motor torque, power, and rotation speed (rpm) during preparation of mechanically milled materials. In addition to assessing the milling process parameters averaged on the time scale comparable to the overall milling time, short-time deviations of these parameters are also considered to help describing milling dynamics. Such time-resolved data affected by ongoing changes in the material properties might be particularly useful when comparing experiments with numerical descriptions of the ball milling process, for example, using a discrete element model.[4,9,10,15]

Table 1. Material Properties of Pure Powders in Comparison to Milling Media[18]

Property	Al	MgO	B_4C	Hardened Steel
Vicker's hardness, MPa	167	660	4980	1700–2300
Shear modulus, GPa	25.9	87–124	192	$\sim$ 80
Poisson's ratio	0.31	0.36	0.21	0.28
Density, g/cc	2.7	3.75	2.51	7.8

Changes in the time-averaged values of real-time indicators are compared to changes in the structure and mechanical properties of the milled materials. Two materials with distinctly different characteristics are selected for this study. Both materials are metal matrix composites consisting of ductile and brittle components. Material compositions are chemically inert; hence no new compounds could have formed affecting the mechanical properties of products. Therefore, work hardening and powder morphology evolving as a result of milling were the only parameters affecting mechanical properties of the prepared composite powders. The brittle components were chosen to have substantially different hardness to investigate its effect on both the milling progress and milling parameters measured in real time.

Experimental

Materials

Prepared composite powders included aluminum, as a ductile component, with inclusions of one of the brittle components: magnesium oxide, MgO, or boron carbide, B_4C. Pure aluminum powder (-325 mesh, 99.9% pure, by Atlantic Equipment Engineers) served as a starting material for the milling. Starting materials for brittle inclusions were magnesium oxide (-325 mesh, 99% pure, by Aldrich Chemical Company, Inc) and boron carbide (<10 Micron Powder, 99% pure, by Alfa Aesar). As was shown in earlier experiments,[4,16,17] during milling, aluminum does not react chemically with either MgO or B_4C, and the milling yields Al·MgO and Al·B_4C dispersion-strengthened composites. The compositions for both materials included 30 wt % of the brittle component. Mechanical properties of the starting components as well as those of the hardened steel milling balls used in experiments are shown in Table 1. The milling media material (hardened steel) is harder than magnesium oxide but is softer than boron carbide.

Milling devices and conditions

An attritor mill by Union Process, model 01HD, was used. The milling vial volume is 750 mL. It is a stationary vial made of hardened steel. A steel impeller rotating at an assigned speed agitates the milling balls. The vial is cooled by room-temperature water. Further details on the geometry of the mill can be found elsewhere.[4]

Case hardened carbon steel balls of 9.5 mm diameter were used. The ball to powder mass ratio was 36, powder mass was 50 g, and the rotation speed of the impeller was 400 rpm. The total milling durations used to prepare the Al·MgO and Al·B_4C composite materials were 4 and 6 h,

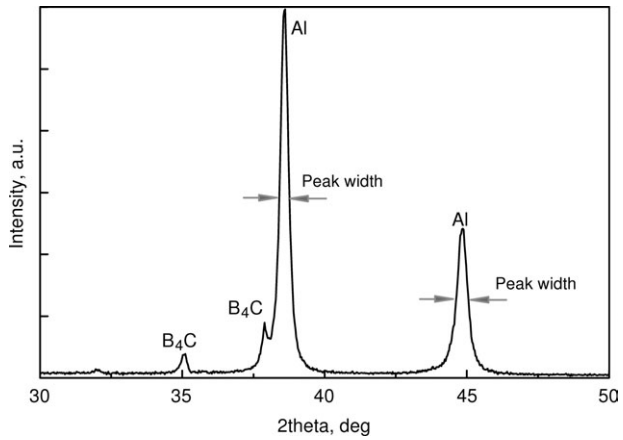

Figure 1. X-ray diffraction pattern for Al·B_4C sample recovered from the attritor mill after 2 h; the FWHM is marked.

respectively. Partially milled samples were recovered every 1-h for mechanical and structural characterization. For some experiments, samples were also recovered and examined in 30-min milling intervals.

Milling progress indicators

Material Characteristics Various material parameters, including particle size, dimensions of the formed inclusions, mechanical characteristics, or crystallographic characteristics can be used as indicators of refinement achieved as a result of milling. In this study, both mechanical and structural characteristics were exploited. Specifically, yield strength measured while preparing consolidated powder samples and a width for an aluminum peak in the x-ray diffraction (XRD) patterns were determined.

In mechanically milled composites, the yield strength typically increases as milling progresses due to formation of dispersion-strengthened materials. The crystallite sizes decrease when the material becomes more refined, for example, as a result of a longer milling time. In the XRD measurements, wider peaks correspond to more refined materials. Hence, an increase in the peak width with time is expected.

The methodology to obtain the yield strength was presented in Ref. [4] and is only briefly outlined here. The powder is compacted in a cylindrical die and the displacement is obtained as a function of the applied load using Instron 5567. The compression curves are replotted in terms of inverse porosity as a function of pressure; obtained trends are interpreted using a modified Heckel equation,[19] in which yield strength is treated as an adjustable parameter.

XRD experiments were performed on a Phillips X'pert MRD powder diffractometer operated at 45 kV and 45 mA using Cu-$K\acute{\alpha}$ radiation ($\lambda = 1.5438$ Å). A typical pattern for the aluminum-boron carbide sample is shown in Figure 1. The peaks for which the widths are indicated belong to the aluminum XRD pattern (38.5° and 44.5°). The peak width is measured at the level equal to half of its maximum height, also known as the full width half max (FWHM). Results for both aluminum peak widths were consistent to each other, so only the FWHM values for the peak at 44.5° are presented.

Real Time Milling Progress Indicators A data acquisition system by Baldor is built in the control unit of the Union Process HD-01 attritor mill. The parameters measured include speed of rotation (rpm), power, and torque. The data were recorded after different milling times in 10-s bursts with 1 ms time resolution. Figure 2 shows typical acquired signals.

Results

Particle shapes and sizes

Powders were recovered every 1-h for both materials and scanning electron microscopy (SEM) images with back-scattered electron detector were taken. The SEM images of samples obtained at certain milling times are presented in Figures 3–5 to illustrate the evolution of the particle shapes. In all images, (a) corresponds to Al·MgO and (b) to Al·B_4C. The pictures on the left and right sides of each figure indicate the same sample shown at two different magnifications (scale shown at the bottom of each image). The milling times are indicated in the top left corner of each picture.

For both materials a qualitatively similar evolution in the particle morphology as a function of milling time is observed. Qualitatively, three steps are identified:

1. Formation of flake-like particles (Figure 3)
2. Breaking down the flakes into smaller, more equi-axial fragments (Figure 4)
3. Agglomeration of the produced fragments into larger particles with relatively stable sizes. (Figure 5)

Within this overall sequence, there were important differences between materials with different compositions. The agglomeration of the broken flake fragments occurred much sooner for Al·B_4C compared to Al·MgO, resulting in the substantially larger dimensions of the stabilized agglomerates of the former compared to latter. Second, the surface of flakes and surface of the formed agglomerated particles was relatively homogeneous for Al·MgO, cf. Figures 3a, 4a and 5a; conversely, inclusions of B_4C were clearly visible at the surface of the Al·B_4C composite particles, Figures 3b, 4b and 5b. Furthermore, unattached B_4C were detected in the Al·B_4C composite material until 1 h of milling Figure 4b, while unattached MgO particles could not be detected in any of the inspected, partially milled samples.

Yield strength

The yield strengths for both prepared composite powders as a function of milling time are presented in Figure 6.

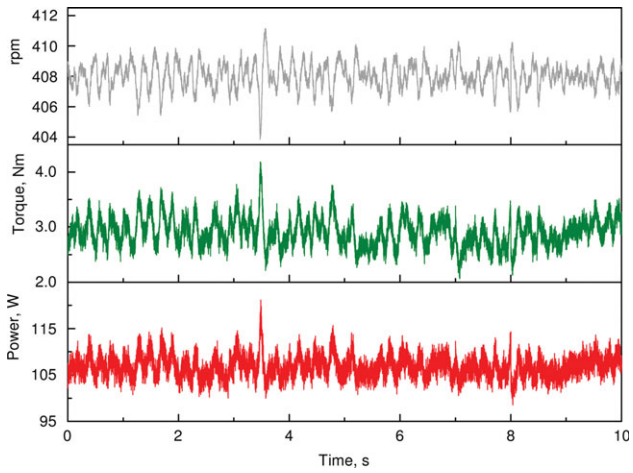

Figure 2. Real-time milling process parameters recorded for an Al·B_4C sample after its 2-h milling.

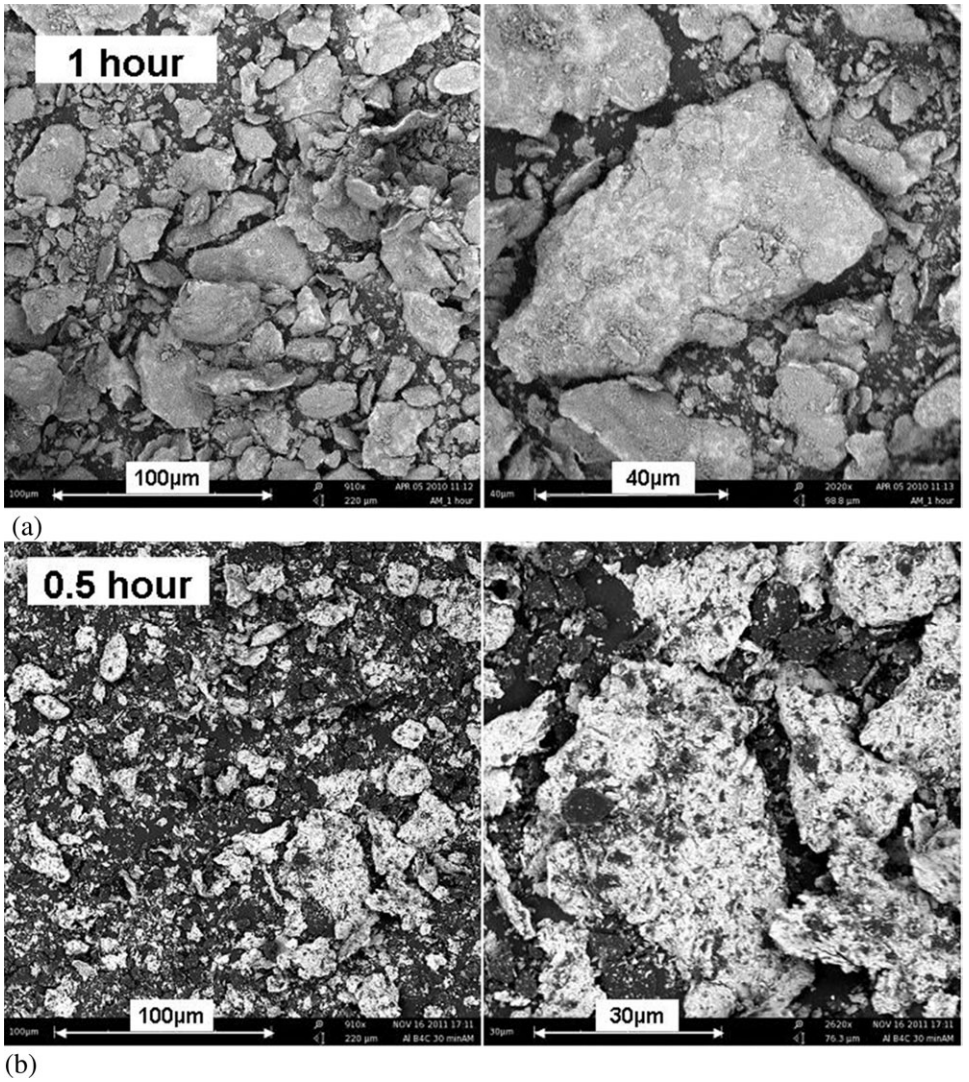

Figure 3. SEM Images Al·MgO (a) and Al·B_4C (b) recovered after 1 h and 0.5 h of milling, respectively.

Each data point is an average of six measurements representing six consolidated pellets for Al·MgO and three measurements/pellets for Al·B_4C. In both the cases, at very short milling times the yield strength is small. This is associated with formation of Al flakes as presented in the SEM images in Figure 3, while aluminum is not yet work hardened. The flakes are readily deformed under pressure, resulting in lower measured yield strength. As the milling continues, the flakes are broken apart and composite particles form. This is accompanied by an increase in the yield strength. This increase is substantial for both materials. Also, upon further milling, the yield strength appears to stabilize for both cases.

X-ray peak width

Figure 7 shows the widths of aluminum peaks or FWHM for the two materials as a function of milling time.

The overall trends in Figure 7 show that the peak width increases as a function of milling time, indicating formation of increasingly more structurally refined materials. The structural refinement appears to occur from the very beginning of the milling process and is unaffected by the formation of flakes at short milling times. For Al·MgO, the refinement of aluminum crystal grains is slower than that for Al·B_4C. Also, the final peak width achieved is greater for Al·B_4C. These observations are likely explained by a greater effectiveness of harder boron carbide inclusions as milling aids accelerating the fracture propagation in the composite particles as compared to softer inclusions of MgO.

Real-time measurements

The fractions of data presented in Figure 2 are shown at an expanded time scale in Figure 8. Changes in power and torque occur in phase with each other whereas changes in rpm occur in the opposite phase. The main period of the observed oscillations, approximately 0.15 s, correlates with the period of the impeller's rotation set at 400 rpm.

At different milling times, average values of the measured power, torque, and rpm changed, and these changes were explored as possible indicators of the milling progress. In addition to the change in the average values of the measured parameters, changes in the amplitudes of their respective oscillations were also noticed. The latter changes were quantified considering standard deviations of the measured parameters taken over a period of 10 s. The processed results of real time measurements for both material systems are shown in Figure 9. The standard deviations in rpm are shown instead of the relatively stable average rpm values. The standard deviations for torque and power follow trends similar to the

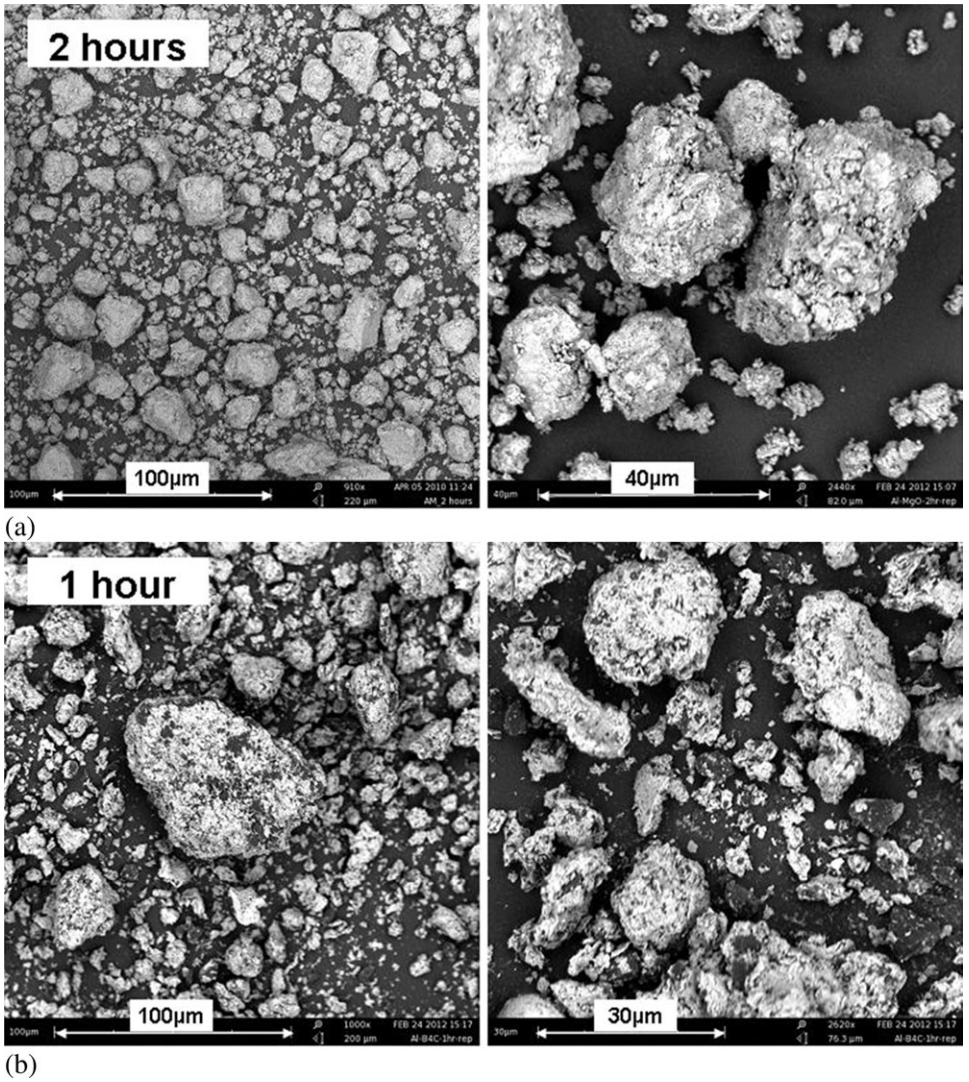

Figure 4. SEM Images Al·MgO (a) and Al·B_4C (b) recovered after 2 h and 1 h of milling, respectively.

standard deviations for rpm and are not plotted for brevity; these standard deviations are represented by the error bars for their respective average values shown in Figure 9.

All three parameters tracked, including power, torque, and standard deviation of rpm, show opposite time-dependent trends for the two materials systems studied. There is an increase in rpm variations, torque and power for the aluminum-magnesium oxide system as a function of the milling time; however, with the exception of the first hour, the same process indicators decrease with milling time for the aluminum-boron carbide composite. Also, despite identical milling conditions, the initial values for all three real time indicators are much higher at the outset for the boron carbide system. This disparity in the trends between the two materials is likely a consequence of the different refinement mechanisms in the two powders. This is turn, is attributed to the difference in properties as shown in Table 1 and discussed below.

Discussion

It is first interesting to directly correlate changes in the powder characteristics, yield strength, and FWHM, with changes in the milling process parameters measured *in situ*. Because measured changes in power, torque, and standard deviation for rpm are well correlated with one another for each material, as shown in Figure 9, only changes in power are taken for direct comparison with yield strength and FWHM. These correlations are shown for both materials in Figure 10. Please note that vertical scales for power are different for different materials.

For Al·MgO composite, changes in all three trends, presented in Figure 10, correlate with one another. As the powder becomes more and more refined and work hardened, the power required to maintain the preset rpm increases. A harder powder also becomes more difficult to compact, as indicated by the increasing yield strength. The increase in FWHM shows a consistent structural refinement as a function of the milling time.

It is interesting that in Figure 10, only changes in yield strength reflect the effect of flake formation at short milling times. From Figure 9 it is apparent that changes in the standard deviation of rpm reflect this effect as well. Although not shown in separate plots, changes in standard deviations for torque and power also correlate with the observed flake formation. Thus, both changes in standard deviations of the milling parameters measured in real time and change in the yield strength are useful in tracking the flake formation for this material.

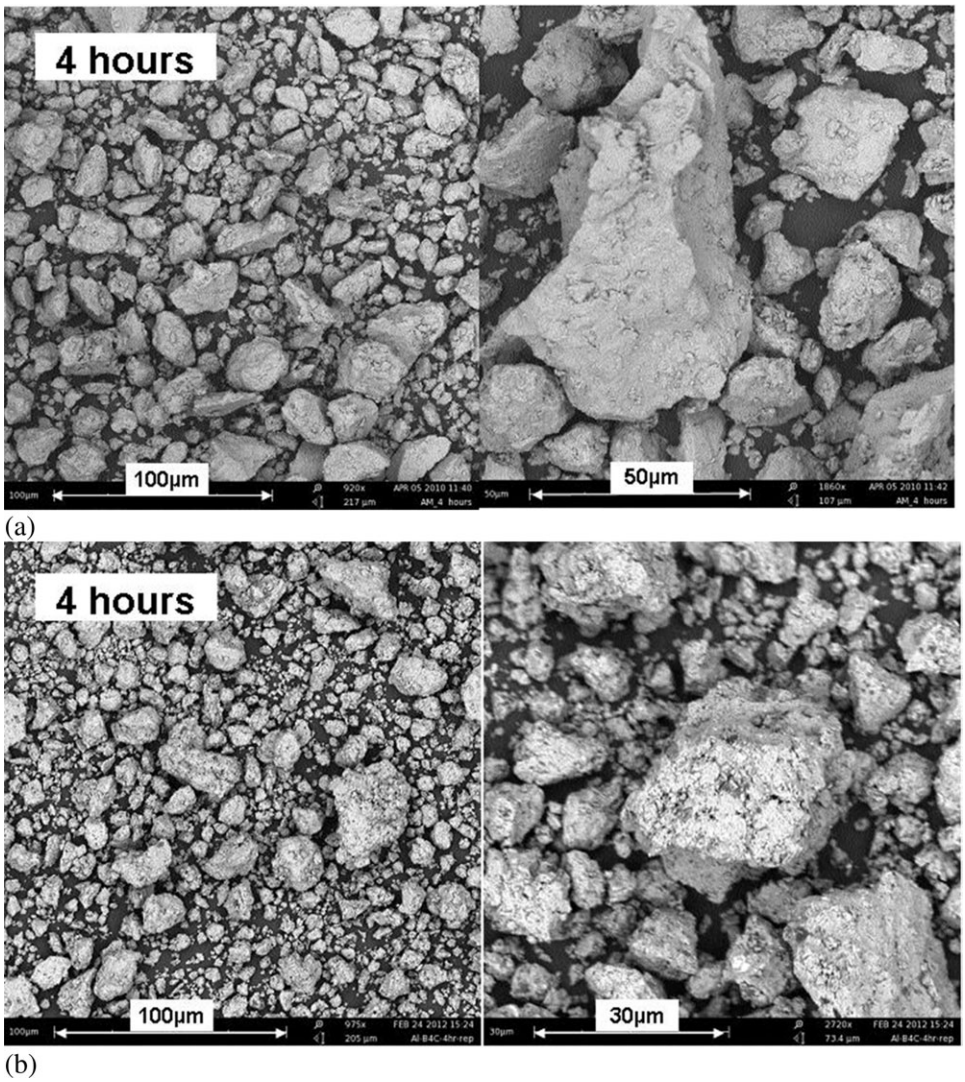

Figure 5. SEM Images Al·MgO (a) and Al·B_4C (b) recovered after 4 h of milling.

For Al·B_4C composite, the power is observed to decrease as a function of the milling time. This may be attributed to the presence of very hard, fine B_4C particles, which behave as an abrasive and create significant friction at earlier times during milling. At longer milling times, when these particles are more and more embedded into Al matrix, their direct interactions with the milling tools are diminished. Apparently, this effect is stronger than that caused by work hardening of the produced Al-matrix composite particles. The yield strength for this powder is affected by changing mechanical properties of the composite particles as well as by changes in the particle shapes. At early milling times, when flakes are formed, the yield strength increase is small because of the ease with which the flakes are deforming.

Effect of flake formation on the measured process parameters may be tracked to the increase in power (as well as torque, and amplitude of oscillations of rpm and other parameters, cf. Figures 9, 10) at short milling times. Embedding abrasive B_4C particles in Al flakes may have caused this effect. For MgO, the flake formation occurred simultaneously with fragmentation of the original MgO particles (not observed in any partially milled samples), while B_4C particles retained their shapes and sizes until much later in the milling process.

The effect of abrasive B_4C particles is less noticeable in the slow compaction, so that the changes in yield strength are dominated by properties of readily deformed Al flakes, similar to Al·MgO.

As soon as the composite particles are produced, the yield strength increases. Its further changes are similar to that of

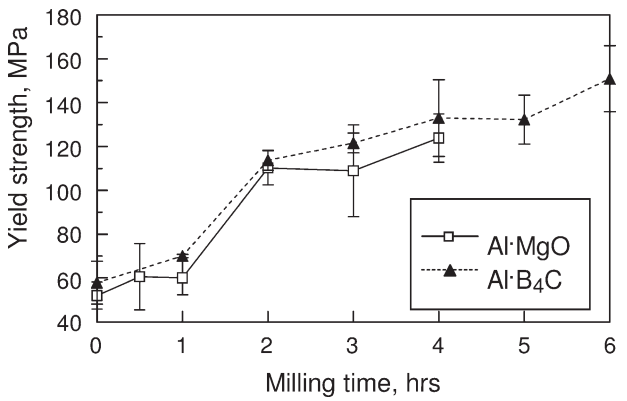

Figure 6. Yield strength for Al·MgO and Al·B_4C samples recovered at different milling times.

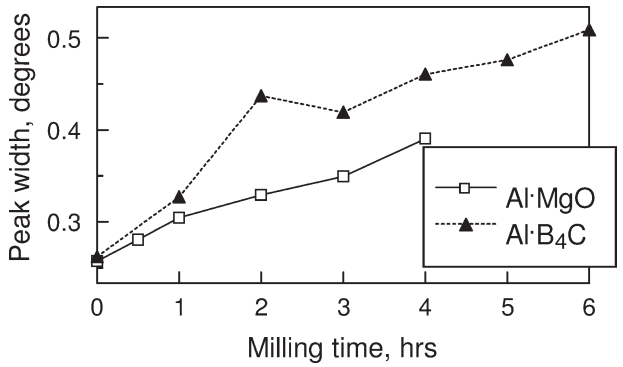

Figure 7. FWHM for aluminum XRD peak at 44.5° as a function of milling time.

Al·MgO composite, that is, due to the formation of work hardened aluminum with tiny embedded boron carbide particles as observed in SEM images. However, the measured in real time power and torque decrease; as mentioned above, likely because of the reduced number of abrasive B_4C particles interacting directly with the milling tools.

A consistent increase in the FWHM shows continuous structural refinement of the Al-based composite material. The rate of this refinement appears to be higher when unattached B_4C particles are present (shorter milling times). The rate is reduced once most of the B_4C particles are embedded; however, the structural refinement continued during the entire experiment.

Changes in the motor power measured in real time (and other real time indicators) as well as changes in XRD pattern as reflected by FWHM and the yield strength and were found to correlate with the structural refinement in this material.

Conclusions

Changes in structural and mechanical characteristics of metal-matrix composite materials prepared by mechanical

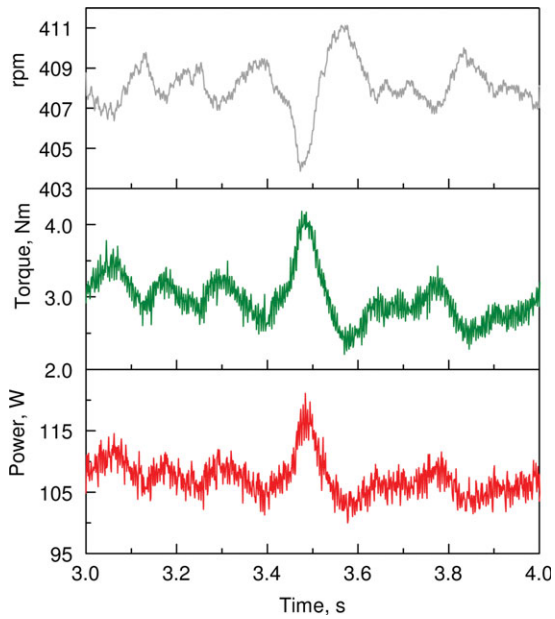

Figure 8. Real-time milling process parameters recorded for an Al·B_4C sample after its 2-h milling (cf. Figure 2) shown with an expanded time scale.

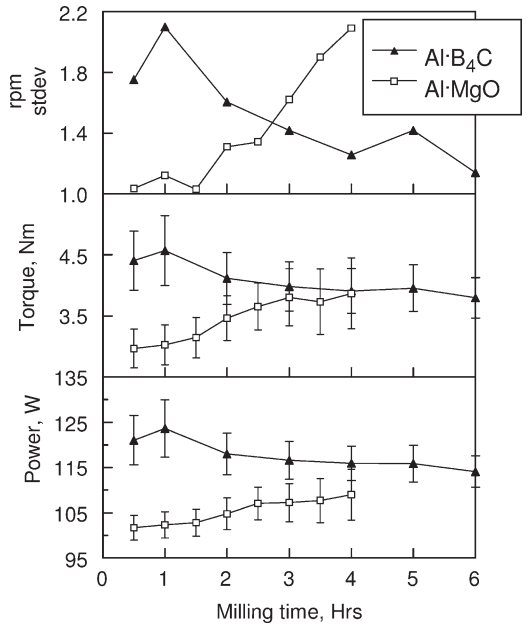

Figure 9. Average values and corresponding standard deviations for real-time indicators measured to assess milling progress as a function of the milling time.

milling and recovered at different milling times are compared to changes in the parameters characterizing milling process in real time. For the material with components softer than the milling media, increasing yield strength, and structural refinement directly correlated with increasing motor power, torque, as well as with increase in the amplitudes of rapid oscillations of all milling process parameters. Without inspecting the partially milled powders, formation of flakes at early milling times can only be unambiguously correlated with changes in the amplitudes of rapid oscillations of the milling process parameters, but not with time-averaged values of these parameters. For the material with a starting component harder than the milling media, the abrasive action of the harder starting particles (becoming less significant at longer milling times) affected the motor power and torque stronger than the hardening of the prepared composite.

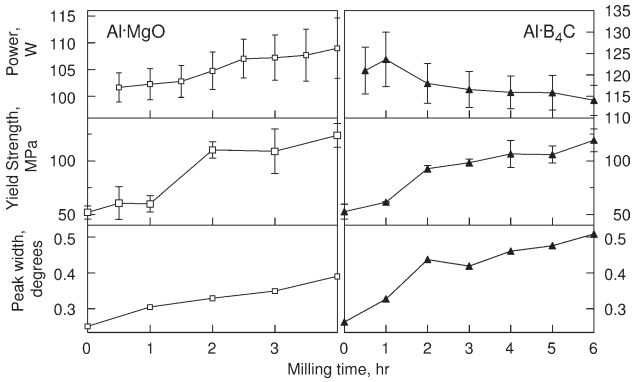

Figure 10. Changes in power measured in real time during ball milling compared to changes in parameters of the powder samples (yield strength and FWHM) recovered at different milling times for Al·MgO and Al·B_4C composites.

Changes in the milling process parameters measured in real time were found useful in tracking the milling progress, although the reduction in the power and torque (as opposed to their increase) correlated with the material refinement. Formation of flakes at early milling times could be correlated with changes in both time-averaged values of power and torque as well as with changes in amplitudes of rapid oscillations of the measured milling process parameters.

Acknowledgments

This work was jointly supported by the U.S. Army and Defense Threat Reduction Agency.

Literature Cited

1. Suryanarayana C. Mechanical alloying and milling. *Prog Mater Sci*. 2001;46:1–184.
2. Yamada K, Koch C. The influence of mill energy and temperature on the structure of the TiNi intermetallic after mechanical attrition. *J Mater Res*. 1993;8:1317–1326.
3. Korchagin MA, Filimonov VY, Smirnov EV, Lyakhov NZ. Thermal explosion of a mechanically activates 3Ni-Al mixture. *Combust Explos Shock Waves*. 2010;46:1317–1326.
4. Santhanam PR, Dreizin EL. Predicting conditions for scaled-up manufacturing of materials prepared by ball milling. *Powder Technol*. 2012;221:403–411.
5. Goodson R, Larson F, Seehan L. Energy input monitoring during attritor milling. *Int J Refract Hard Met*. 1985;4:165–169.
6. Kimura H, Kimura M, Takada F. Development of an extremely high energy ball mill for solid state amorphizing transformations. *J Less-Common Met*. 1988;140:113–118.
7. Iosanna A, Magini M. Power measurements during mechanical milling, an experimental way to investigate the energy transfer phenomena. *Acta Mater*. 1996;44:1109–1117.
8. Magini M, Colella C, Iasonna A, Padella F. Power measurements during mechanical milling-II, the case of "single path cumulative" solid state reaction. *Acta Mater*. 41998;6:2841–2850.
9. Ward TS, Chen W, Schoenitz M, Dave RN, Dreizin EL. A study of mechanical alloying processes using reactive milling and discrete element modeling. *Acta Mater*. 2005;53:2009–2918.
10. Jiang X, Trunov MA, Schoenitz M, Dave RN, Dreizin EL. Mechanical alloying and reactive milling in a high energy planetary mill. *J Alloys Compd*. 2009;478:246–251.
11. Mulas G, Schiffini L, Cocco G. Impact energy and reactive milling: a self propagating reaction. *Mater Sci Forum*. 1997;235–238:15–22.
12. Rydin RW, Maurice D, Courtney TH. Milling Dynamics: part I, Attritor dynamics, Results of a cinematographic study. *Metall Trans*. 1993;A24:175–185.
13. Shoshin YL, Mudryy RD, Dreizin EL. Preparation and characterization of energetic Al-Mg mechanical alloy powders. *Combust Flame*. 2002;128:259–269.
14. Schoenitz M, Ward TS, Dreizin EL. Preparation of energetic metastable nano-composite materials by arrested reactive milling. *Mater Res Soc Symp Proc*. 2004;800:AA2.6.1–AA2.6.6.
15. Feng YT, Han K, Owen DRJ. Discrete element simulation of the dynamics of high energy planetary ball milling processes. *Mater Sci Eng*. 2004;A375:815–819.
16. Khakbiz M, Akhlaghi F. Synthesis and structural characterization of Al-B4C nano-composite powders by mechanical alloying. *J Alloys Compd*. 2009;479:334–341.
17. Mohammad Sharifi E, Karimzadeh F, Enayati MH. Fabrication and evaluation of mechanical and tribological properties of boron carbide reinforced aluminum matrix nanocomposites. *Mater Des*. 2011;32:3263–3271.
18. Shacketford JF, Alexander W. *CRC Material Science and Engineering Handbook*, 3rd ed. Boca Raton, FL: CRC Press, 2000.
19. Denny J. Compaction equations: a comparison of Heckel and Kawakita equations. *Powder Technol*. 2002;127:162–172.

Manuscript received Apr. 27, 2012, and revision received July 19, 2012.